To the Graduate Council:

I am submitting herewith a thesis written by Richard B. Smith entitled "The Inverse Gamma Model in Field Oriented Control". I have examined the final copy of this thesis for form and content and recommend that it be accepted in partial fulfillment of the requirements for the degree of Master of Science, with a major in Electrical Engineering.

J. Milton Bailey

J. Milton Bailey, Major Professor

We have read this thesis
and recommend its acceptance:

J M Googe

J M Bailey

F. V. Symonds

Accepted for the Council:

C W Minkel

Associate Vice Chancellor
and Dean of the Graduate School

STATEMENT OF PERMISSION TO USE

In presenting this thesis in partial fulfillment of the requirements for a Master's degree at the University of Tennessee, Knoxville, I agree that the Library shall make it available to borrowers under rules of the Library. Brief quotations from this thesis are allowable without special permission, provided that accurate acknowledgement of the source is made.

Permission for extensive quotation from or reproduction of this thesis may be granted by my major professor, in his absence, by the Head of Interlibrary Services when, in the opinion of either, the proposed use of the material is for scholarly purposes. Any copying or use of the material in this thesis for financial gain shall not be allowed without my written permission.

Signature Richard B. Smith

Date May 1, 1992

THE INVERSE GAMMA MODEL IN FIELD ORIENTED CONTROL

A Thesis

Presented for the

Master of Science

Degree

The University of Tennessee, Knoxville

Richard B. Smith

May 1992

ABSTRACT

In order to control a three-phase induction motor in a similar fashion to that of a DC machine, the induction motor equivalent circuit must be analyzed in terms of torque and field current quantities. This paper develops the Inverse Gamma model as an alternative equivalent circuit model for the induction motor and uses it to illustrate how torque and flux quantities can be independently controlled. The concept of field oriented control is explained using characteristics of this model. A simple, indirect field oriented control diagram is developed and simulated.

TABLE OF CONTENTS

LIST OF FIGURES

1. Introduction

For use in quick response, high-performance variable speed applications, the DC motor has been the popular choice. Because of its design, the armature current and field flux can be controlled independently of one another. This control allows varation of the motor speed under most load torque conditions. As an example, the separately excited DC motor operating with a constant torque load can have its speed controlled by holding the field flux constant and varying the armature current.

Although it has excellent controllability, the DC motor has its disadvantages. The same brushes and commutator that provide decoupled field flux and armature current control also reduce the motor's reliability and require extra maintenance. The DC motor is usually heavier than the AC induction motor and generally costs more.

The induction motor is much less popular for variable speed applications because its AC source is difficult to control. Although more reliable, lighter, and durable, the induction motor has been primarily used in applications where speed control is not important.

Due to recent advances in power semiconductor technology, better control of AC voltage, current, and frequency is available. Control of these parameters makes it possible to generate the motor voltages and currents necessary for independently controlling the field and torque quantities of the induction motor.

The conventional equivalent circuit model of the induction motor does not easily lend itself to the analysis of the motor in terms of torque and field flux currents. With proper modifications, the conventional equivalent circuit can be altered to represent the motor in terms of independent field and torque currents. This modified circuit is known as the Inverse Gamma circuit model. Using this model, an output torque equation in terms of the field and torque input currents can be found. This equation is found to resemble the torque equation of the separately excited DC motor.

The generation and decoupled control of the field and torque current components for the induction motor are achieved using a method known as field oriented control. This control strategy constructs a single current vector from the desired torque and field flux currents and "orients" the field component of the vector with the rotating rotor flux vector of the motor. This oriented vector is then converted into the three-phase supply currents.

To illustrate this control strategy, a simple steady state block diagram of an indirect field oriented control scheme of an induction motor is simulated. The simulation is performed given a constant torque load on the motor. The field flux current component is kept constant while the speed is varied by changing the torque current component. This type of speed control is found to be similar to that of the separately excited DC motor.

2. Characteristics of DC and Induction Motors

2.1 The DC Motor

Because of simple control methods, DC motors have been the preference in applications where quick torque response and speed control are needed. The mechanical construction of the DC motor and its commutator provides decoupled control of armature and field currents. This control enables independent variation of torque and field flux current within the motor. To illustrate this, consider the circuit diagram in Figure 2.1-1* of a separately excited DC motor.

When the shaft is rotating at speed ω, the back e.m.f. of the motor E_g, is given by

$$E_g = K_g \phi \omega \qquad (2.1\text{-}1)$$

where Φ is the magnetic field flux and K_g is a constant based on properties of the particular machine. The output torque of the machine is given by

$$T = K_g \phi I_a \qquad (2.1\text{-}2)$$

where I_a is the armature current. Since $\Phi = KI_f$ where K is a constant, the output torque can also be expressed in the form

$$T = K' I_f I_a \qquad (2.1\text{-}3)$$

where K' is K_g multiplied by K. The output torque is now expressed as a function of

* This figure and all subsequent figures are contained in the Appendix

field current I_f and armature current I_a.

To illustrate the torque and speed control in the separately excited DC motor, consider again the circuit of Figure 2.1-1. The voltage loop equation of the armature circuit can be written as

$$V_t = I_a R_a + E_g \tag{2.1-4}$$

Rewriting equation 2.1-2 in terms of I_a gives

$$I_a = \frac{T}{K_t \phi} \tag{2.1-5}$$

Substituting equation 2.1-1 and 2.1-5 into equation 2.1-4 gives

$$V_t = \frac{T}{K_g \phi} R_a + K_g \phi \omega \tag{2.1-6}$$

By keeping the field flux Φ constant, the two terms $R_a/K_g\Phi$ and $K_g\Phi$ can also be treated as constants. A general graph of equation 2.1-6 with constant Φ is shown in Figure 2.1-2 by displaying torque and speed combination for different values of V_t.

In the graph, it can be seen that for a given load torque T_L, the speed is varied by simply varying the terminal voltage V_t. It can also be observed that any torque and speed operating point can be attained by keeping the flux Φ fixed and adjusting V_t. Since varying V_t is essentially the same as varying I_a, one can conclude that controlling I_a while holding I_f constant will produce any torque and speed combination desired.

This ability to independently vary field current and armature current provides excellent control of the DC motor. Unfortunately, the same mechanical structure which allows for the decoupling of field and armature current using mechanical brushes consequently weighs more, has higher rotor inertia, and demands more maintenance than that of the induction motor.

2.2 Three-Phase Induction Motors

One of the most widely used motors in industry is the induction motor. It has a simple, durable structure and boasts low cost and high reliability. Unlike the DC motor, the rotor circuit of the induction motor is isolated from the stator circuit which eliminates the problem of brushes. Induction motors can have single-phase or multi-phase windings. The three-phase induction motor is most widely studied for variable speed applications and is the subject of this discussion.

The three-phase induction motor contains stator windings which produce a rotating magnetic flux when supplied from a balanced three-phase AC source. The speed ω of this rotating magnetic flux in a P pole pair machine supplied by an AC source of angular frequency ω_e is given by

$$\omega = \frac{\omega_e}{P} \qquad (2.2\text{-}1)$$

This rotating magnetic field "induces" a current in the closed rotor windings by transformer action. It is the interaction of the induced rotor current and the rotating magnetic flux which produces torque.

Two particularly important parameters in describing the operation of the induction motor are the stator angular frequency ω_e and the per unit slip S. This slip is a function of the electrical angular speed of the rotor shaft rotation ω_o, stator angular frequency ω_e, and is calculated by

$$S=\frac{\omega_e-\omega_o}{\omega_e} \tag{2.2-2}$$

The angular frequency of the current induced in the rotor circuit, ω_r, is

$$\omega_r=\omega_e-\omega_o \tag{2.2-3}$$

and is referred to as the slip frequency. This allows the slip to be expressed as

$$S=\frac{\omega_r}{\omega_e} \tag{2.2-4}$$

To illustrate the induction motor circuit behavior, consider the induction motor phase equivalent circuit diagram shown in Figure 2.2-1 [1] where:

R_s = Stator Primary Resistance

L_{ls} = Stator Leakage Inductance

L_{ms} = Stator Self-inductance

L_m = Mutual Inductance

N_{sr} = Stator to Rotor Turns Ratio at given rotor speed

L_{mr}' = Rotor Self-inductance referred to the Rotor

L_{lr}' = Rotor Leakage Inductance referred to the Rotor

r_r' = Rotor Resistance referred to the Rotor

The left side represents the stator circuit, which operates at the stator frequency ω_e. The right side of the circuit represents the rotor circuit, which operates at rotor slip frequency ω_r. The stator and rotor circuits are coupled by transformer action with a ratio of the stator to rotor turns ratio N_{sr}. Writing the voltage loop equation for the rotor circuit gives

$$I_r^{\prime}(r_r^{\prime}+j\omega_r L_{lr}^{\prime})+E_r^{\prime}=0 \tag{2.2-5}$$

Making use of equation 2.2-4, ω_r can be written as

$$\omega_r=S\omega_e \tag{2.2-6}$$

Substituting equation 2.2-6 into equation 2.2-5 and dividing by S gives

$$I_r^{\prime}(\frac{r_r^{\prime}}{S}+j\omega_e L_{lr}^{\prime})+\frac{E_r^{\prime}}{S}=0 \tag{2.2-7}$$

Using equation 2.2-7, the modified circuit of Figure 2.2-1 is shown in Figure 2.2-2 with the rotor and stator circuits operating at the same frequency ω_e.

Two equivalent ways to represent a magnetically coupled circuit of turns ratio 1:1 and mutual inductance M are shown in Figure 2.2-3. The two winding form is shown on the left and the "T" form is shown on the right.

In order to take advantage of this transformation, we will define $r_r = (N_{sr})^2 r_r^{\prime}$, $L_{mr} = (N_{sr})L_{mr}^{\prime}$, and $L_{lr} = (N_{sr})^2 L_{lr}^{\prime}$, which allows us to present the rotor parameters referred to the stator. Letting $L_s = L_{ms} + L_{ls}$ and $L_r = L_{mr} + L_{lr}$, the transformation illustrated in Figure 2.2-3 is modified giving the steady state induction motor equivalent circuit model of Figure 2.2-4. This equivalent circuit is commonly referred to as the "T" form and is widely used in induction motor analysis. The circuit parameters are generally found using machine terminal measurements during no load and locked rotor conditions. Although this equivalent circuit appears simpler, it does not lend itself well to the analysis of the division of stator current I_s into I_m and I_r components.

The induction motor has its mechanical advantages over the DC motor. Unfortunately, the equivalent circuit model is much more complicated in terms of analyzing torque and field current quantities. Using some modifications, this model can be transformed into a more useful circuit.

3. Inverse Gamma Model and Field Oriented Control

3.1 Inverse Gamma Model

To aid in the understanding of the stator current division into flux producing current and torque producing current, an approximate steady state and transient model is needed. To develop this, consider first the familiar "T" form equivalent circuit for an induction motor shown in Figure 3.1-1 with

R_s = Primary Resistance

L_s - L_m = Primary Leakage Inductance

L_r - L_m = Secondary Leakage Inductance

L_m = Magnetizing Inductance

r_r = Rotor Resistance

S = Slip

The voltage equation for the left hand loop is given by

$$V_s = I_s R_s + j\omega_e (L_s - L_m) I_s + j\omega_e L_m (I_s + I_r) \tag{3.1-1}$$

Simplifying:

$$V_s = I_s (R_s + j\omega_e L_s) + j\omega_e L_m I_r \tag{3.1-2}$$

The voltage equation for the right hand loop is given by

$$0 = I_r \frac{r_r}{S} + j\omega_e (L_r - L_m) I_r + j\omega_e L_m (I_r + I_s) \tag{3.1-3}$$

Simplifying:

$$0 = I_r\left(\frac{r_r}{s} + j\omega_e L_r\right) + j\omega_e L_m I_s \tag{3.1-4}$$

Now consider the general equivalent circuit illustrated in Figure 3.1-2 with nonzero constant a. The voltage equation for the left hand loop can be written as

$$V_s = I_s R_s + j\omega_e (L_s - aL_m) I_s + j\omega_e a L_m \left(I_s + \frac{I_r}{a}\right) \tag{3.1-5}$$

Simplifying:

$$V_s = I_s(R_s + j\omega_e L_s) + j\omega_e L_m I_r \tag{3.1-6}$$

The voltage equation for the right hand loop can be written as

$$0 = \frac{I_r}{a}\left(a^2 \frac{r_r}{s}\right) + j\omega_e (a^2 L_r - aL_m) \frac{I_r}{a} + j\omega_e a L_m \left(\frac{I_r}{a} + I_s\right) \tag{3.1-7}$$

Simplifying and dividing each side by a gives

$$0 = I_r\left(\frac{r_r}{s} + j\omega_e L_r\right) + j\omega_e L_m I_s \tag{3.1-8}$$

Since equations 3.1-2 & 3.1-6 and 3.1-4 & 3.1-8 are identical, the circuit given in Figure 3.1-2 can be used to represent the induction motor in the steady state. If we choose constant a to be L_m/L_r, the rotor inductance will become zero and the circuit will be of the Inverse Gamma form, as shown in Figure 3.1-3.

The equivalent circuit in Figure 3.1-3 allows us to subdivide the stator current I_s into orthogonal reactive flux producing current $I_{s\phi}$ and resistive torque producing current I_{st}. Referring to the Inverse Gamma circuit in Figure 3.1-3, the steady state current $I_{s\phi}$ can be calculated by

$$I_{s\Phi}=\frac{\frac{L_m}{L_r}E_r}{j\omega_e(\frac{L_m}{L_r})L_m}=\frac{E_r}{j\omega_e L_m} \tag{3.1-9}$$

In Figure 3.1-1, the voltage E_r is the voltage across r_r/s. Referring to the transient equivalent circuit in Figure 3.1-4, this voltage E_r is also equal to the time rate of change of the rotor flux Φ_r. In the steady state:

$$E_r=j\omega_e\Phi_r \tag{3.1-10}$$

Substituting equation 3.1-10 into equation 3.1-9 gives

$$I_{s\Phi}=\frac{\Phi_r}{L_m} \tag{3.1-11}$$

indicating the steady state rotor flux is proportional to $I_{s\Phi}$.

The output torque T_e of the motor represented by the circuit in Figure 3.1-1 is a function of the power in the resistor r_r/S [2]. This torque can be expressed as

$$T_e=3\frac{P}{2}\frac{(I_r)^2 r_r}{\omega_e S}=3\frac{P}{2}\frac{E_r(-I_r)}{\omega_e} \tag{3.1-12}$$

where ω_e is the synchronous supply frequency. The current I_{st} in figure 3.1-3 is

$$I_{st}=-\frac{L_r}{L_m}I_r \tag{3.1-13}$$

Writing equation 3.1-13 in terms of I_r and equation 3.1-9 in terms of E_r and substituting the results into equation 3.1-12 gives

$$T_e=3\frac{P}{2}\frac{(j\omega_e L_m I_{s\Phi})(-(-\frac{L_m}{L_r}I_{st}))}{\omega_e}=3\frac{P}{2}\frac{L_m^2}{L_r}|I_{s\Phi}||I_{st}| \tag{3.1-14}$$

This equation illustrates how the output electrical torque of the induction motor is expressed in terms of the torque current I_{st} and the orthogonal flux current $I_{s\Phi}$ by representing the motor in terms of the Inverse Gamma equivalent circuit. This equation 3.1-14 closely resembles the torque equation for a separately excited DC motor.

The general transient equivalent circuit with nonzero constant a for an induction motor is shown in Figure 3.1-4, where Φ_r = rotor flux [1]. By choosing a = L_m/L_r, the circuit will become the Transient Inverse Gamma form shown in Figure 3.1-5.

Being equivalent to the "T" form circuit model of the induction motor, the Inverse Gamma form model makes it possible to analyze the equivalent circuit in terms of flux producing current $I_{s\Phi}$ and torque producting current I_{st}. The output torque can also be calculated in terms of these two currents and is analogous to that of a separately excited DC motor. This circuit will also prove helpful in determining the governing equations for field oriented control.

3.2 Vector Control

The Inverse Gamma model equivalent circuit simplifies the analysis and study of the induction motor in terms of flux and torque producing current. The independent control of these two currents is best explained graphically using the d-q axis theory of modeling [3]. This type of modeling transforms the three phase supply current vectors into one single current vector. This single vector is represented in a direct (d) and quadrature (q) axis coordinate system with the d axis as the vertical axis and the q axis as the horizontal axis. The d axis represents the flux component of the vector and the q axis represents the torque component of the vector.

The d-q model can be represented in either the stationary reference frame or the rotating reference frame. In the stationary reference frame, the d and q axes are fixed. In the rotating reference frame, the d and q axes rotate at the synchronous speed of the motor. When studied in the rotating reference frame, sinusoidal quantities can be treated as steady state D.C. quantities.

The orthogonal torque current and flux current I_{st} and $I_{s\phi}$ from the Inverse Gamma model lend themselves well to this d-q model by their representation in the d-q coordinate system as i_{qs} and i_{ds} respectively. The desired motor torque and flux current at any instant can be represented by a single vector in the rotating d-q reference frame. Figure 3.2-1 shows the torque producing current i_{qs} leading the flux producing current i_{ds} by 90 degrees. The conversion of these two currents into the vector I_s and angle Θ are also shown. By varying the angle and magnitude of the vector I_s, the i_{ds} and i_{qs} components can be independently varied. This type of control is referred to as vector control [3].

Figure 3.2-2 shows how the torque component i_{qs} can be increased to i_{qs}' while the flux component i_{ds} remains the same by increasing the magnitude of I_s to I_s' and changing the vector angle Θ to Θ' [3]. Figure 3.2-3 shows how the flux component i_{ds} can be increased to i_{ds}' while the torque component i_{qs} can remain the same by again varying the magnitude and vector angle of I_s [3].

From the illustrations of Figure 3.2-2 and 3.2-3, it is shown that any combination of orthogonal flux and torque producing current magnitudes can be resolved into its own unique vector magnitude and angle. Changing the vector magnitude I_s and angle Θ results in a corresponding change in i_{ds} and i_{qs}. The magnitude is calculated by

$$|I_s| = \sqrt{i_{ds}^2 + i_{qs}^2} \tag{3.2-1}$$

and angle by

$$\theta = \arctan\frac{i_{qs}}{i_{ds}} \tag{3.2-2}$$

3.3 Field Orientation

Once the desired torque and flux current magnitudes are resolved into the correct vector and angle, another condition must be met. The desired current vector will need to be positioned so that the flux producing current component i_{ds} is always aligned with the revolving rotor flux of the motor. This alignment is best described using the diagram in Figure 3.3-1.

In this diagram, the d^s and q^s axes are stationary and the d^e and q^e axes rotate at synchronous angular velocity ω_e. For any given time t, the angle Θ_e between the synchronously rotating axes and stationary axes is $\omega_e t$ and is equivalent to the sum of the rotor angle Θ_r and slip angle Θ_{sl}. The slip angle Θ_{sl} is equal to $\omega_r t$ and the mechanical rotor angle Θ_r is equal to $\omega_0 t$. The current vector I_s and angle Θ are also shown with respective i_{ds} and i_{qs} components. The rotor flux Φ_r is shown aligned with the rotating d^e axis. It can be seen in this figure that the i_{ds} component of I_s is coincident with the rotor flux Φ_r. This indicates proper field orientation of I_s.

To maintain proper field orientation, the position of the d^e axis must be identified at all times during operation. By calculating Θ_r and Θ_{sl}, the d^e axis can be located and the instantaneous angle of the current vector I_s can be calculated by adding Θ, Θ_r, and Θ_{sl}. The angle Θ is determined by equation 3.2-2 and the mechanical rotor angle Θ_r is computed by measuring and integrating the rotor shaft speed ω_o. The slip angle Θ_{sl}, however, is not easily measured but can be calculated from Inverse Gamma equivalent circuit characteristics.

Consider once again the steady state Inverse Gamma equivalent circuit of Figure 3.1-3. It can be observed that the division of stator current I_s into I_{st} and $I_{s\phi}$ can be written as

$$I_{st} = -\frac{L_r}{L_m} I_r = I_s \frac{j\omega_e \frac{L_m^2}{L_r}}{\frac{L_m^2}{L_r^2}\frac{r_r}{s} + j\omega_e \frac{L_m^2}{L_r}} \tag{3.3-1}$$

Substituting $S = \omega_r/\omega_e$ and simplifying gives

$$I_r = -I_s \frac{jL_m \omega_r}{r_r + j\omega_r L_r} \tag{3.3-2}$$

which indicates the division of stator current is governed by the slip angular velocity

ω_r. In this case, ω_r can be determined by the division of I_s into I_{st} and $I_{s\Phi}$. Equating the voltage magnitudes across the magnetizing branch and the rotor circuit branch in Figure 3.1-3 gives

$$\omega_e \frac{L_m^2}{L_r} I_{s\Phi} = \frac{L_m^2}{L_r^2} \frac{r_r}{s} I_{st} \tag{3.3-3}$$

Again, letting $S = \omega_r/\omega_e$ and simplifying yields

$$\omega_r = \frac{I_{st}}{I_{s\Phi}} \frac{r_r}{L_r} = \frac{I_{st}}{I_{s\Phi}} \frac{1}{T_r} \tag{3.3-4}$$

where $T_r = L_r/r_r$. Letting $I_{st} = i_{qs}$ and $I_{s\Phi} = i_{ds}$, equation 3.3-4 can be written as

$$\omega_r = \frac{i_{qs}}{i_{ds}} \frac{1}{T_r} \tag{3.3-5}$$

which gives the slip angular frequency ω_r for a given T_r, i_{qs} and i_{ds}. This will be useful in field orientating the vector I_s.

Once the vector I_s and the angles necessary for correct field orientation have been calculated, it is desirable to convert this polar current vector into three instantaneous phase motor currents; i_a, i_b, and i_c. If we consider that, at any instant, the rotating sinusoidal current distribution in the motor can be transformed into a single polar vector $\underline{I}_s$ by

$$I_s = \frac{2}{3}(i_a + i_b e^{j\frac{2\pi}{3}} + i_c e^{j\frac{4\pi}{3}}) \tag{3.3-6}$$

and inversely transformed by

$$i_a = RE(\underline{I}_s)$$

$$i_b = RE(\underline{I}_s e^{j\frac{2\pi}{3}}) \qquad (3.3\text{-}7)$$

$$i_c = RE(\underline{I}_s e^{j\frac{4\pi}{3}})$$

then the inverse transformation in equation 3.3-7 can be used to convert the vector $\underline{I}_s$ and angle Θ into three-phase supply currents.

3.4 Block Diagram

An elementary block diagram of the field orientation control scheme is shown in Figure 3.4-1 [1]. The desired i_{qs} and i_{ds} commands are first computed by the torque and flux calculator. These i_{qs} and i_{ds} components are then converted into the vector I_s and angle Θ by the vector calculator according to equations 3.2-1 and 3.2-2. To field orient this vector I_s, the rotor angle Θ_r and slip angle Θ_{sl} must be added to the vector angle Θ as shown in Figure 3.3-1. The rotor angle Θ_r is found by integrating the measured rotor shaft speed ω_o. The slip angle Θ_{sl} is determined by integrating the slip frequency ω_r. In this diagram, ω_r is computed from equation 3.3-5 using i_{qs}, i_{ds}, and the rotor time constant T_r. Once the vector I_s and angle $\Theta + \Theta_r + \Theta_{sl}$ necessary to field orient this vector have been determined, the three motor supply currents can be generated using equation 3.3-7.

By controlling the magnitude and angle of the vector resultant of i_{ds} and i_{qs}, independent control of the orthogonal torque and flux producing currents can be achieved. The flux producing current component of I_s must then be aligned with the rotating rotor flux of the motor in order to effectively control the motor by changing the i_{qs} and i_{ds} commands. This alignment is accomplished by computing the necessary angle to offset the vector I_s. This angle is a function of the desired i_{ds} and i_{qs} commands, rotor shaft speed, and machine electrical characteristics. To illustrate this, a simple control block diagram was used to show how the vector is calculated and then oriented to control the motor.

4. Computer Model and Simulation

Given a control block diagram and the appropriate governing relationships derived from the Inverse Gamma circuit model, a computer simulation of a field oriented control system can be performed for an induction motor using LABVIEW, a visual programming language. With this simulation, steady state motor speeds for a constant torque load can be changed by applying a constant i_{ds} input and varying the i_{qs} input. Comparing the different results will demonstrate that speed control of the induction motor with a constant torque load is very similar to that of the separately excited DC motor described earlier.

To illustrate the concept of field oriented control of an induction motor, LABVIEW programming language was selected for this simulation. LABVIEW programming allows the user to simulate a system by constructing its block diagram on the screen. Each block of the block diagram performs a specific type of mathematical operation. A block can be chosen from a library of different functions or created by the user to incorporate a group of functions. The inputs and outputs for each of these blocks are then connected to perform the desired simulation. A "control panel" is a separate screen used to input values to the block diagram as well as observe output values. The inputs and outputs of the "control panel" are represented in the block diagram as special blocks and are connected as desired.

LABVIEW elements are designed to handle data one sample at a time. To represent operation over a period of time t, the period can be divided into i intervals of width t/i by using i+1 sample points. To include the time element in the simulation, the inputs and outputs to the system are represented by one dimensional arrays of n samples. The block diagram can then be selected to perform n iterations. Feedback is performed by retaining the (n)th value of the desired feedback element and using it in the (n+1)th iteration as feedback. The number of elements in the arrays is selected by the user and represents a specified period of time. The output array can then be displayed numerically or graphically.

There are many advantages to visual programming. By constructing the system in block diagram form, the user is able to visualize the system modeled. An otherwise complicated system can be broken down into different subsystems for simplicity. Troubleshooting the system is made simple by checking the individual blocks. Within the system, different nodes can be monitored for comparison with other nodes and system input values can be quickly and easily changed.

To demonstrate operation of the induction motor using field oriented control, an approximate model of the block diagram in Figure 3.4-1 is constructed in LABVIEW. Since the objective is to illustrate operation of the induction motor by keeping i_{ds} fixed and varying i_{qs}, the input torque and flux calculator used in Figure 3.4-1 are omitted and i_{ds} and i_{qs} are used as inputs to the system. By keeping i_{ds} constant, the motor can be represented in the steady state by equation 3.1-14 with i_{ds} and i_{qs} as inputs and torque T_e as the output. The LABVIEW block diagram of the field oriented control system is shown in Figure 4.0-1.

This model begins with the input d^e - q^e rotating reference frame currents i_{ds}

and i_{qs} and converts them into the vector I_s and angle Θ. Adding the instantaneous slip angle Θ_{sl} and the rotor angle Θ_r to Θ places the vector and its new angle ($\Theta + \Theta_{sl} + \Theta_r$) in the d^s - q^s stationary reference frame. At this point, the three instantaneous motor currents can be generated using equation 3.3-7. Since the induction motor is to be modelled in terms of steady state i_{ds} and i_{qs} current vectors rotating at the synchronous angular velocity of the motor, the stationary reference frame vector I_s and angle ($\Theta + \Theta_{sl} + \Theta_r$) are converted to orthogonal i_{dss} and i_{qss} currents. This is accomplished by transforming the vector I_s and angle ($\Theta + \Theta_{sl} + \Theta_r$) into d and q components. These stationary reference frame currents, i_{dss} and i_{qss}, are then converted into i_{ds} and i_{qs} rotating reference frame currents for use as input motor currents.

The induction motor model determines the motor slip frequency ω_r' and motor output angular acceleration α as a function of i_{ds} and i_{qs}, motor parameters, and load torque T_l. This angular acceleration is integrated to give the rotor angular velocity ω_o. The value of ω_o is the output of the system and is also fed back for determining the rotor angle Θ_r. The motor slip frequency ω_r' is used as feedback for converting the stationary frame currents into rotating frame currents.

For the sake of simplicity, the control system and motor model make use of different subroutines. These subroutines are represented by other squares within the block diagram and can be created by the user or taken from a library of "stock" subroutines within LABVIEW. The "stock" LABVIEW subroutines used in the program are the rectangular-to-polar and polar-to-rectangular conversion functions.

These are used for converting the i_{ds} and i_{qs} to the vector I_s and angle Θ and transforming the field oriented vector and its angle to their stationary reference frame i_{dss} and i_{qss} currents. The custom subroutines created for this simulation are the slip calculator, stationary-to-rotating (S/R) reference frame conversion, integrator, and induction motor model.

The slip calculator subroutine is illustrated in Figure 4.0-2. The inputs to the calculator are i_{ds}, i_{qs}, L_r, and r_r. The output of the slip calculator ω_r is calculated according to equation 3.3-5 with $T_r = L_r/r_r$. This subroutine is used to calculate the slip angular frequency from the input command currents and is included in the motor subroutine to calculate the motor slip angular frequency ω_r'.

The stationary-to-rotating (S/R) reference frame conversion subroutine is illustrated in Figure 4.0-3. It is used to convert the two input currents i_{dss} and i_{qss} from the stationary d^s - q^s reference frame into the equivalent rotating frame d^e - q^e output currents i_{ds} and i_{qs}. This operation is shown graphically in Figure 3.3-1. The output currents are referenced to the d^e - q^e axis, which rotates at the synchronous angular speed ω_e of the induction motor. If the angle Θ_e between the stationary d^s - q^s axis and the rotating d^e - q^e axis is known, the d^e - q^e rotating frame currents i_{ds} and i_{qs} are found using the following equations:

$$i_{qs} = i_{qss}\cos\theta_e - i_{dss}\sin\theta_e \tag{4.0-1}$$

$$i_{ds} = i_{qss}\sin\theta_e + i_{dss}\cos\theta_e \tag{4.0-2}$$

This subroutine uses equations 4.0-1 and 4.0-2 for generating the output i_{ds} and i_{qs}

currents.

The integrator subroutine shown in Figure 4.0-4 is used throughout the simulation. One application is for integrating the motor output angular acceleration α to produce the output motor rotor angular velocity ω_o. The other application of the integrator is integrating the sum of the slip angular velocity and rotor shaft angular velocity ($\omega_r + \omega_o$) for determining the sum of the slip angle and rotor angle (Θ_{sl} + Θ_r).

The integrator uses as inputs the array element, the element index, the total number of samples in the array, and the amount of time in seconds represented by the array. Using the present input value inp(k) and the previous input value inp(k-1), the integral is approximated using the trapezoidal rule with the following equation:

$$out(k) = out(k-1) + \frac{inp(k) + inp(k-1)}{2} \, \frac{seconds}{samples} \tag{4.0-3}$$

Equation 4.0-3 is the governing equation in the block diagram of the integrator subroutine shown in Figure 4.0-4. In this subroutine, the first iteration of the block diagram is initialized with all previous values set equal to zero. This is shown by the shaded window in Figure 4.0-4. When the index is zero, the previous value inputs are set equal to zero. When the index is nonzero, the previous values are used in the equation.

The steady state induction motor model subroutine is illustrated in Figure 4.0-5 and has three primary functions. The first function is to calculate the motor output torque T_e in terms of i_{ds} and i_{qs}. The next function is to calculate the output angular acceleration α from the motor output torque T_e, moment of inertia J, and total motor load torque. The final function is to generate the motor slip frequency ω_r. The motor output torque T_e is determined from i_{ds} and i_{qs} using equation 3.1-14. The total load torque is calculated outside of the motor subroutine and is the sum of the given motor load torque T_l and the damping torque $B\omega_o$. The total load torque is subtracted from the motor output torque and the difference is divided by J to give the output angular acceleration α. Another output of the motor subroutine is the motor slip frequency $\omega_r^{/}$. The value of $\omega_r^{/}$ is calculated from the input i_{ds} and i_{qs} motor currents using the slip calculator subroutine described earlier. This output slip frequency is fed back for use in the stationary-to-rotating vector conversion subroutine.

The objective of this simulation is to model an indirect field oriented control system of an induction motor and observe the output rotor shaft speed, given a constant torque load and different input command currents. To achieve this, the LABVIEW block diagram of Figure 4.0-1 is used with actual motor parameters. It is shown that the output rotor shaft speed of the motor under a constant torque load can be changed by holding the input current i_{ds} constant and varying the i_{qs} input current. In each simulation, the same values are used for i_{ds}, T_l, B, L_r, r_r, and J. The number of samples used in each simulation is 10,000, which represents a time period of 10 seconds.

This simulation is performed twice, using two different steady state values of i_{qs} and the same steady state value of i_{ds} to illustrate the difference in steady state rotor shaft speed magnitude for each case. The simulation is again performed given a constant i_{ds} input and a varying i_{qs} input to illustrate the rotor shaft speed change relative to the change in the input current i_{qs}. It is shown that the change in rotor shaft speed closely follows the change in i_{qs}.

The motor parameters used in these simulations are taken from a 5 horsepower, 4 pole, 460 volt, 6.5 amp, three phase induction motor [4] with the following characteristics:

r_s = 1.18 ohms

L_s = 308 millihenries

L_r = 308 millihenries

r_r = 1.09 ohms

L_m = 301 millihenries

J = 0.038 kg - m^2

Using the above characteristics, the magnetizing current i_{ds} is found by

$$i_{ds}=\frac{V_{\phi-n}}{\omega_e(L_s+L_m)} = 1.156\ amps \qquad 4.0\text{-}4$$

With a full load current i_{fl} of 6.5 amps, the current i_{qs} at full load is found to be

$$i_{qs}=\sqrt{(i_{fl})^2-(i_{ds})^2} = 6.396\ amps \qquad 4.0\text{-}5$$

The first simulation uses as inputs the full load i_{ds} and i_{qs} currents and a load torque of 2 n-m. The graph of the output rotor shaft speed versus time for these currents is shown on the LABVIEW "control panel" in Figure 4.0-6. The steady state rotor shaft speed for this case is observed to be approximately 1150 rpm. The next simulation is shown in Figure 4.0-7 and performed with the same value for i_{ds}, but with the i_{qs} current lowered to 5.5 amps. Given the same amount of load, the steady state rotor shaft speed in Figure 4.0-7 is approximately 950 rpm which is much less than the 1150 rpm observed in Figure 4.0-6. The objective of these two comparisons is to show the difference in output speed for different i_{qs} currents.

The result of the next simulation is shown in Figure 4.0-8. In addition to the graph of the output speed versus time, a graph of the input i_{qs} current versus time is displayed beneath the graph of the output speed. During this simulation, the magnitude of i_{ds} is kept constant while full load i_{qs} is applied during the first 5 seconds of operation and then negative full load i_{qs} is applied for the remaining 5 seconds of operation. The graph of the output speed and the input i_{qs} current together reveals the output speed closely follows the input i_{ds} current command.

Comparing the steady state output speed in the first two simulations reveals that speed control of the induction motor under indirect field oriented control is similar to that of the separately excited D.C. motor. The response of the motor speed to the sudden change in i_{qs} in Figure 4.0-8 indicates the usefulness of a field oriented control system in an application where quick speed response is desirable.

To verify the operating characteristics of field oriented control of an induction motor, the governing equations and appropriate block diagram can be modelled on the computer. Using a visual programming language such as LABVIEW serves to better illustrate the block diagram of the entire field oriented control system. The LABVIEW program can be subdivided into subroutines for simplicity and illustrations of the system's different components and their purposes. Once the program is placed into operation, the control system and motor can be simulated with different input currents to observe the output rotor speed under different input conditions. By keeping the i_{ds} current fixed, the simulation shows the output rotor speed under a constant torque load is varied by changing the i_{qs} magnitude. This control is found to be similar to that of the separately excited D.C. motor.

5. Conclusion

Control of the separately excited DC motor is simple and versatile due to the fact that the motor field flux and armature current are independent inputs and can be independently controlled. An analysis of the equivalent circuit for the separately excited DC motor illustrates how the rotor shaft speed of the motor under a constant torque load can be varied by simply varying the motor armature current and maintaining a constant field flux.

The AC induction motor has mechanical advantages over the DC motor because of its design. The absence of brushes and commutator in the AC motor enhances its reliability and reduces its cost and weight. The disadvantage of the AC motor is its poor controllability. In order to properly control the induction motor, complete control of the input AC to the motor must be achieved.

Progress in the power semiconductor and microprocessor control fields has made control of AC voltage, current, and frequency available for controlling the AC motor. With this flexibility, the induction motor can be studied with the objective of operating it like a separately excited DC motor. The conventional equivalent circuit of the induction motor does not adequately represent the motor in terms of field flux and armature (torque) current. By making a few modifications, the conventional equivalent circuit can be transformed into the Inverse Gamma equivalent circuit. This equivalent circuit represents the motor in terms of orthogonal torque and flux producing currents.

Varying the flux and torque producing currents is accomplished by creating a current vector from the two orthogonal currents and changing the magnitude and phase angle of this input current vector. The flux producing component of the vector is then "oriented" with the rotating field flux of the motor using a method known as field oriented control. Once the desired current vector is known, it can then be transformed into the three motor supply currents.

In order to demonstrate this type of control, the field oriented control block diagram is developed and modeled in the steady state. Modeling of the block diagram is performed on a personal computer using LABVIEW, a visual programming language. The modeling is performed for an induction motor with constant torque load, given a constant field flux current input and different torque current inputs. Observing the rotor speed for each case demonstrates a similarity between field oriented control of the induction motor and the control of a separately excited DC motor.

LIST OF REFERENCES

LIST OF REFERENCES

[1] Ohm, Dal, "Field Oriented Control of Induction Motors" *Motion*, March/April 1991.

[2] Novotney, D.W., et al. (Editor) "Introduction to Field Orientation and High Performance AC Drives," IEEE IAS Tutorial Course, 1986.

[3] Bose, B.K. , "Power Electronics and AC Drives," Prentice Hall, 1986

[4] Lorenz, Robert, Yang, Sheng Ming, "Efficiency-Optimized Flux Trajectories for Closed Cycle Operation of Field Oriented Induction Machine Drives," *Conference Record, IEEE/IAS Annual Meeting*, 1988

APPENDIX

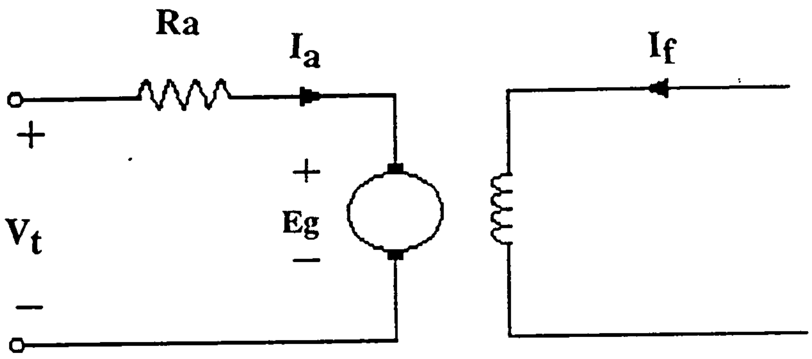

Figure 2.1-1. Separately Excited DC Motor Diagram

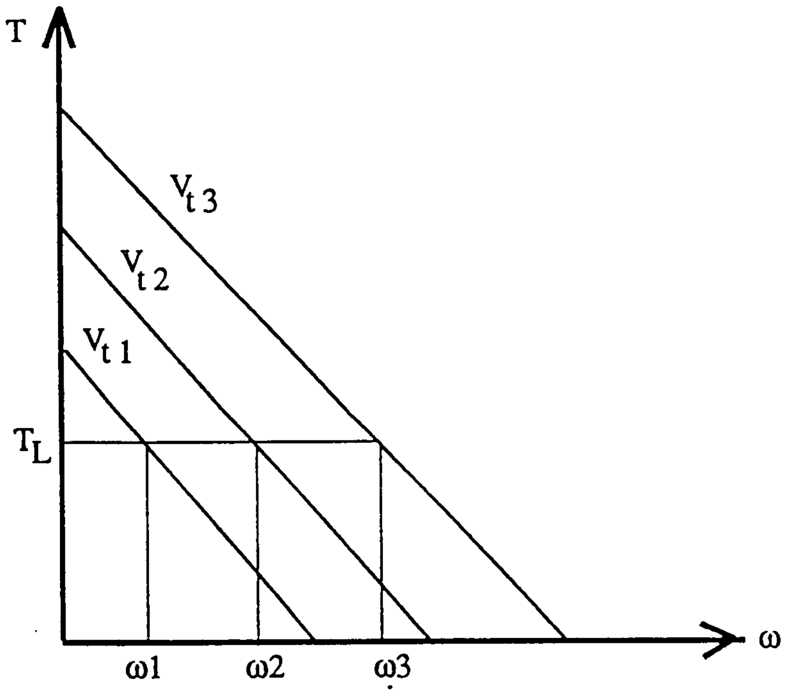

Figure 2.1-2 Torque/Speed Graphs for $V_{t1} < V_{t2} < V_{t3}$

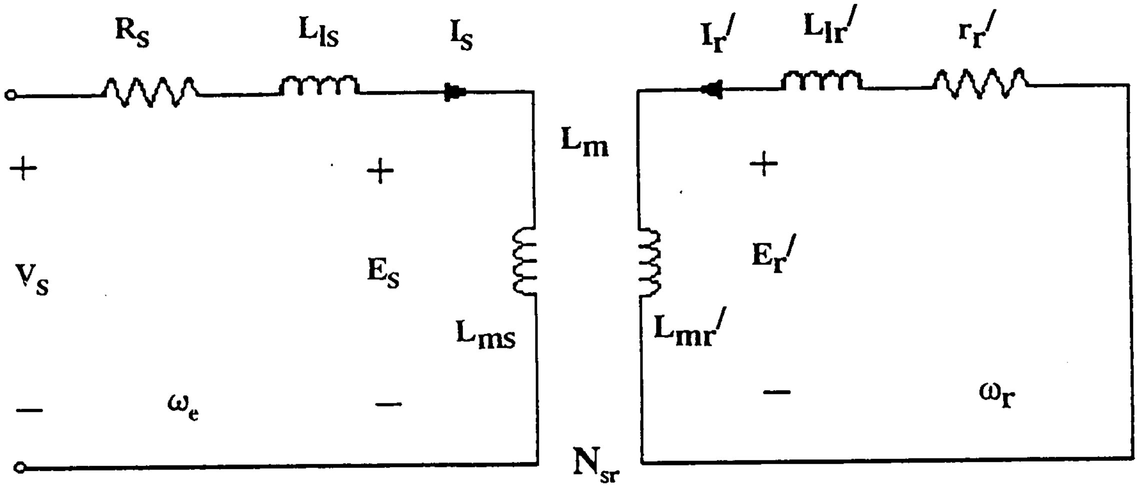

Figure 2.2-1 Induction Motor per phase Circuit Diagram

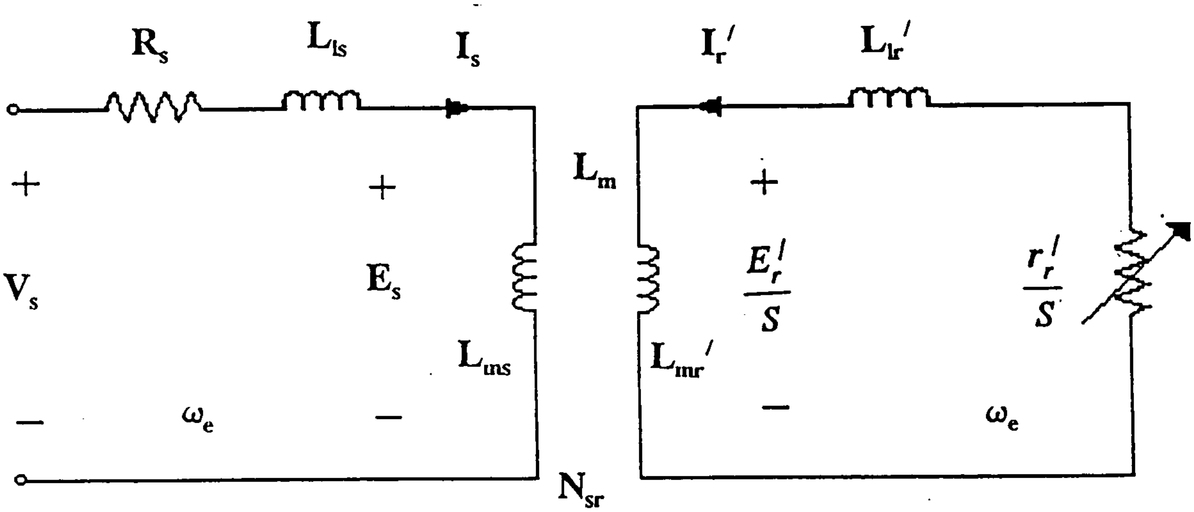

Figure 2.2-2 Equivalent Induction Motor per phase Circuit Diagram

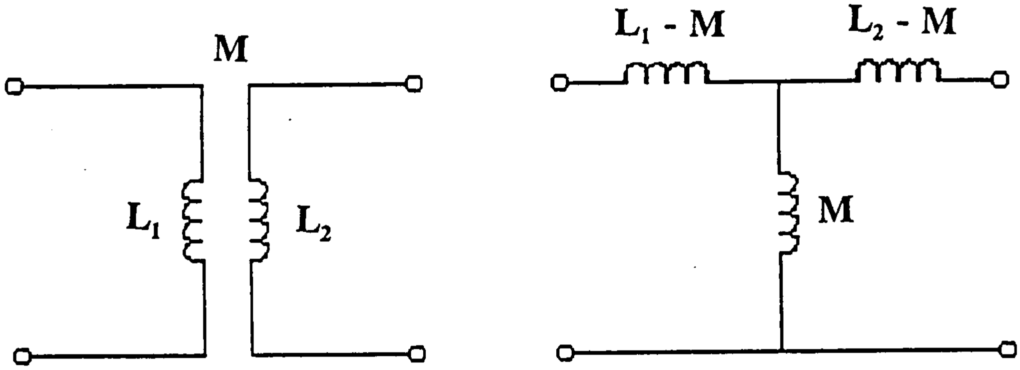

Figure 2.2-3 Two Winding Magnetic Circuit Equivalents

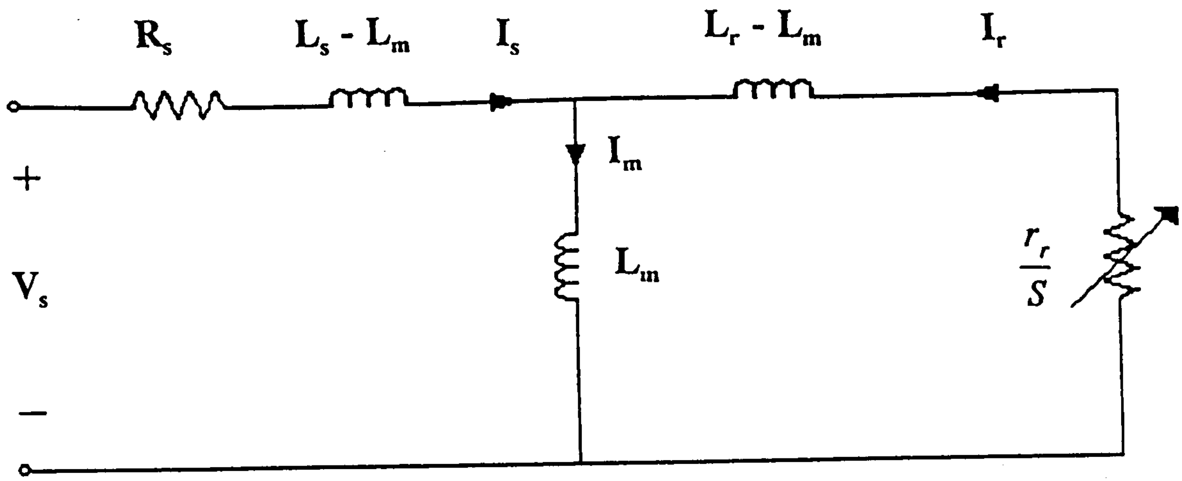

Figure 2.2-4. Induction Motor Equivalent Circuit

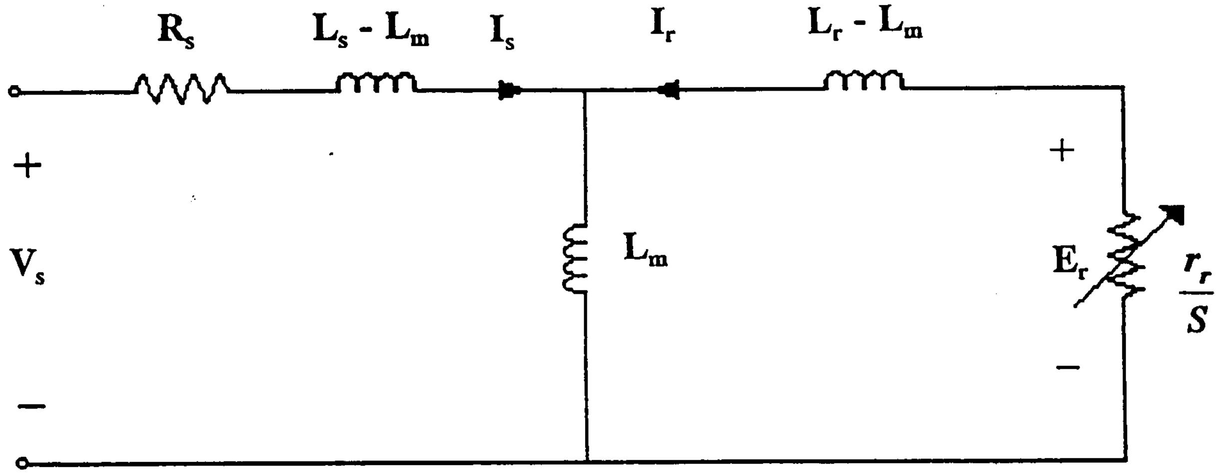

Figure 3.1-1 Steady State "T" Form Model

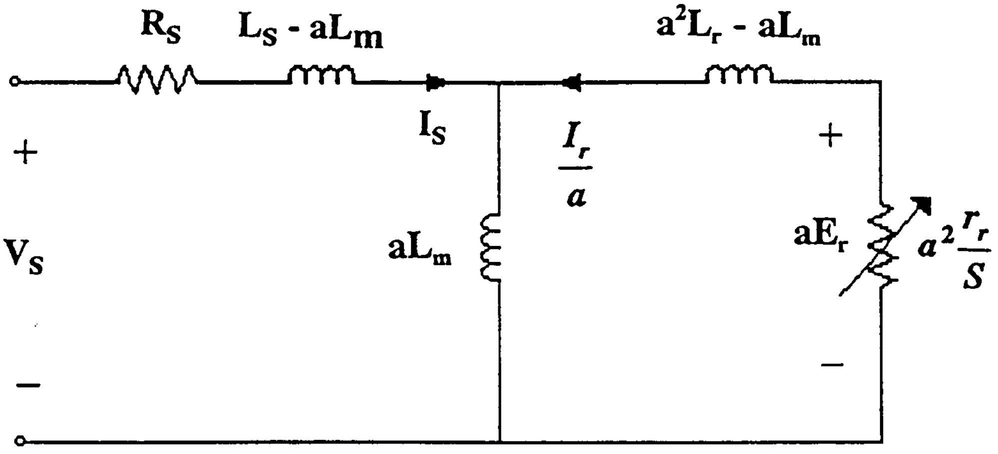

Figure 3.1-2. "T" Form Equivalent Circuit with Constant a

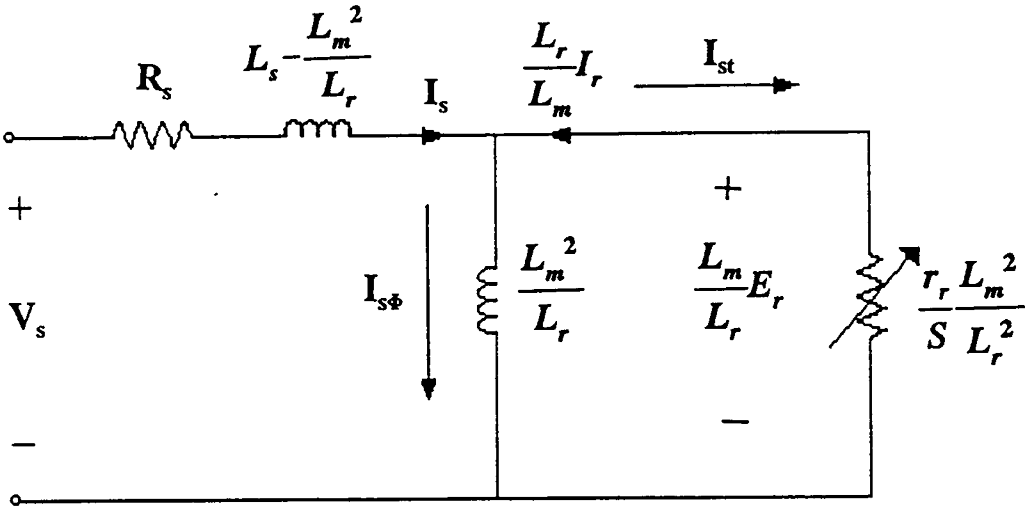

Figure 3.1-3. Steady State Inverse Gamma Equivalent Circuit

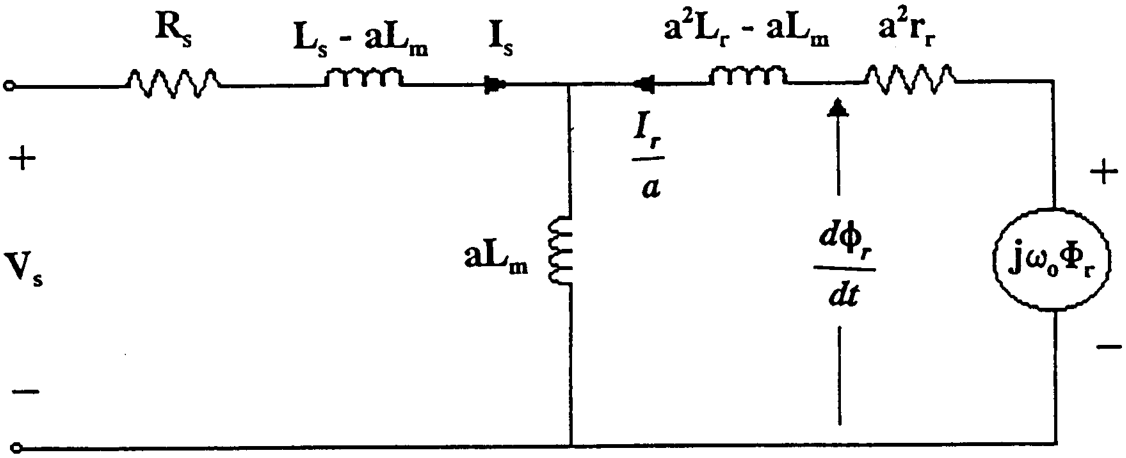

Figure 3.1-4. Transient Equivalent Circuit with Constant a

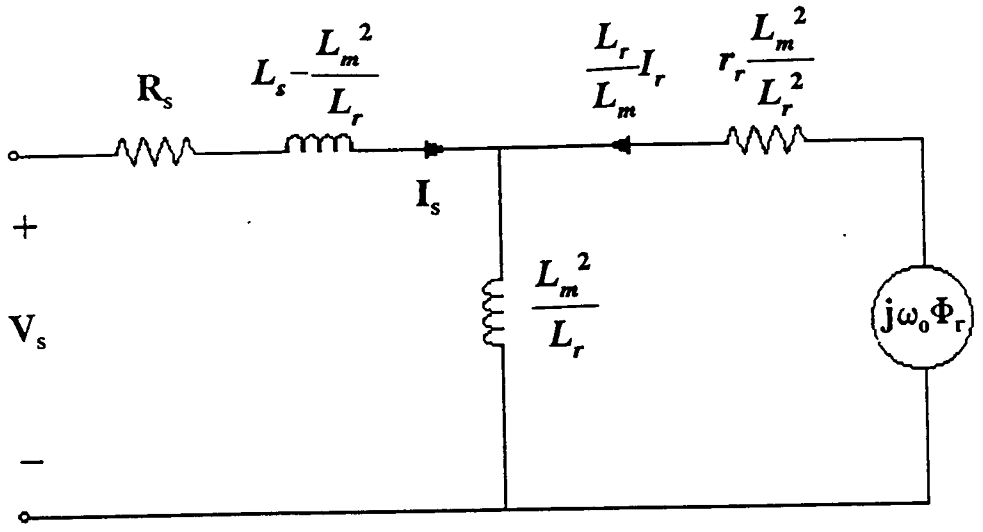

Figure 3.1-5 Transient Inverse Gamma Equivalent Circuit

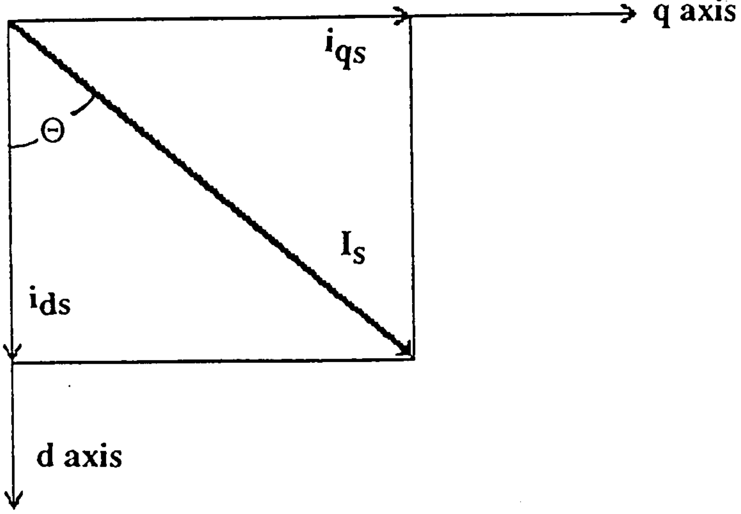

Figure 3.2-1. Resolution of i_{qs} and i_{ds} into Vector I_s

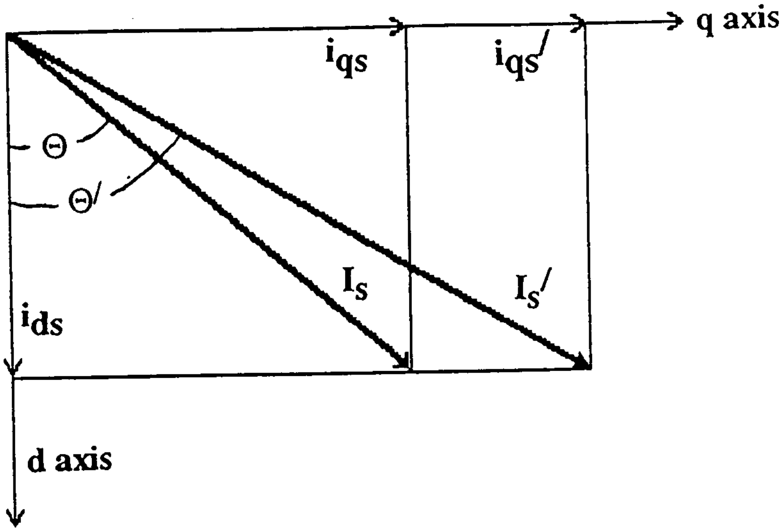

Figure 3.2-2. Increase of Torque Current i_{qs} to i_{qs}'

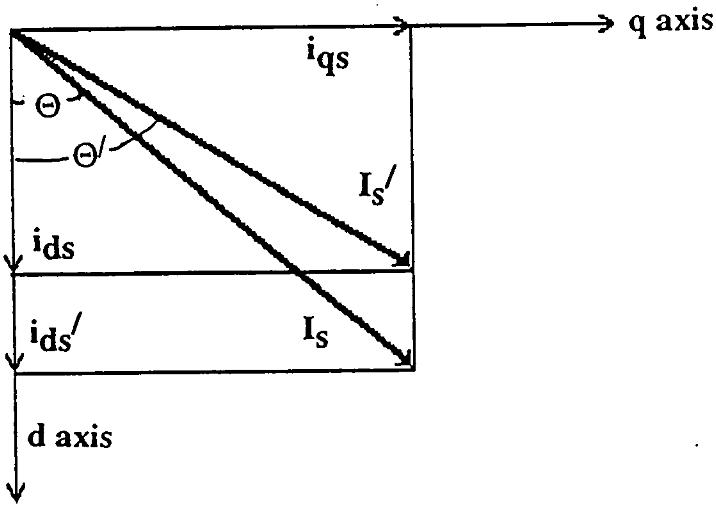

Figure 3.2-3. Increase of Flux Current from i_{ds} to i_{ds}'

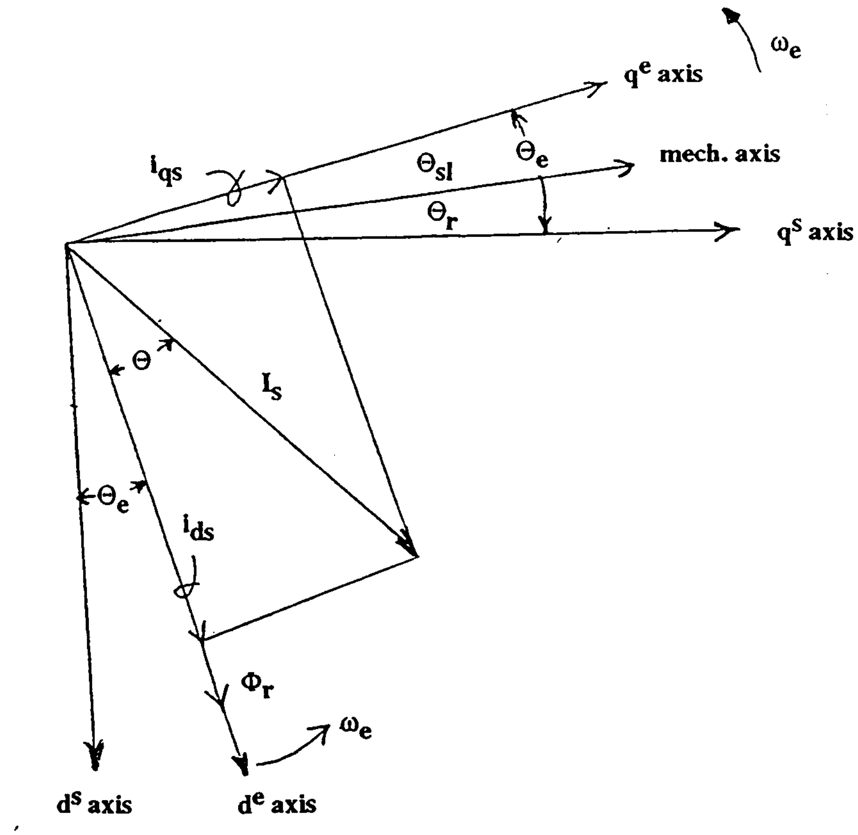

Figure 3.3-1. Phasor Diagram Showing Correct Field Orientation

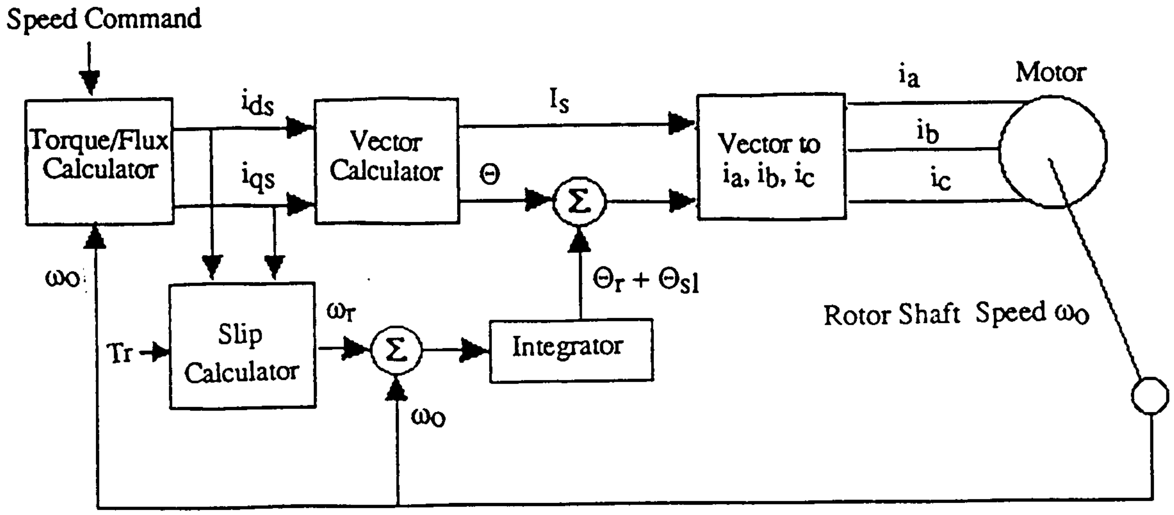

Figure 3.4-1. Indirect Field Orientation Control Block Diagram

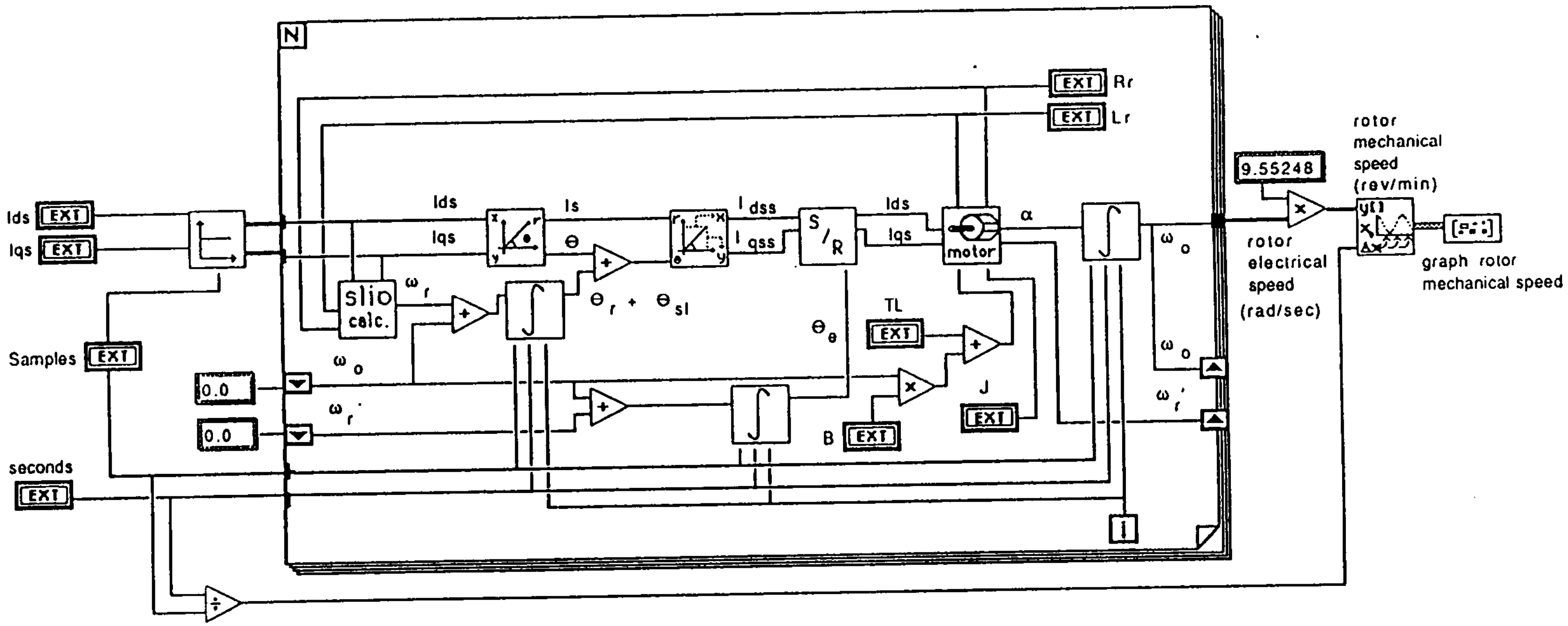

Figure 4.0-1. Field Oriented Control System

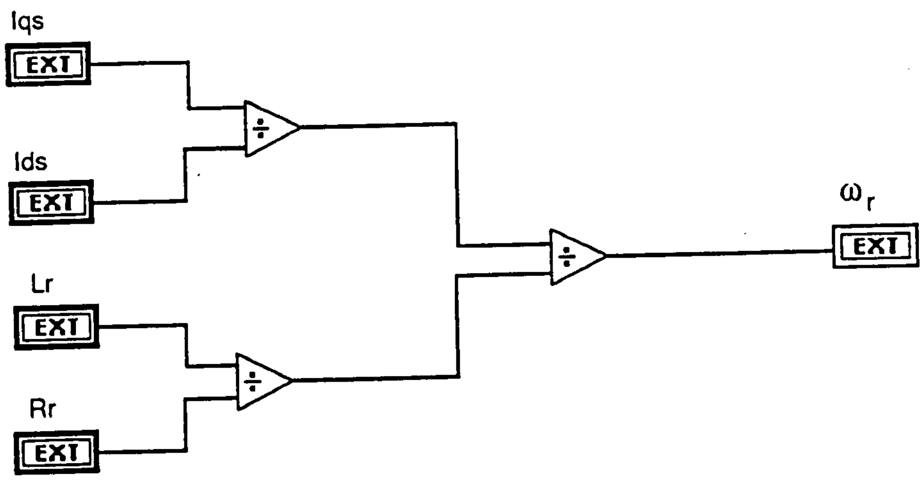

Figure 4.0-2. Slip Calculator Subroutine

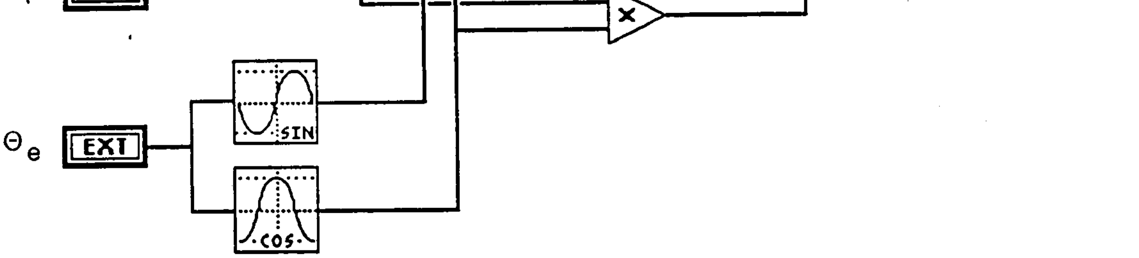

Figure 4.0-3. Stationary-to-Rotating Reference Frame Conversion Subroutine

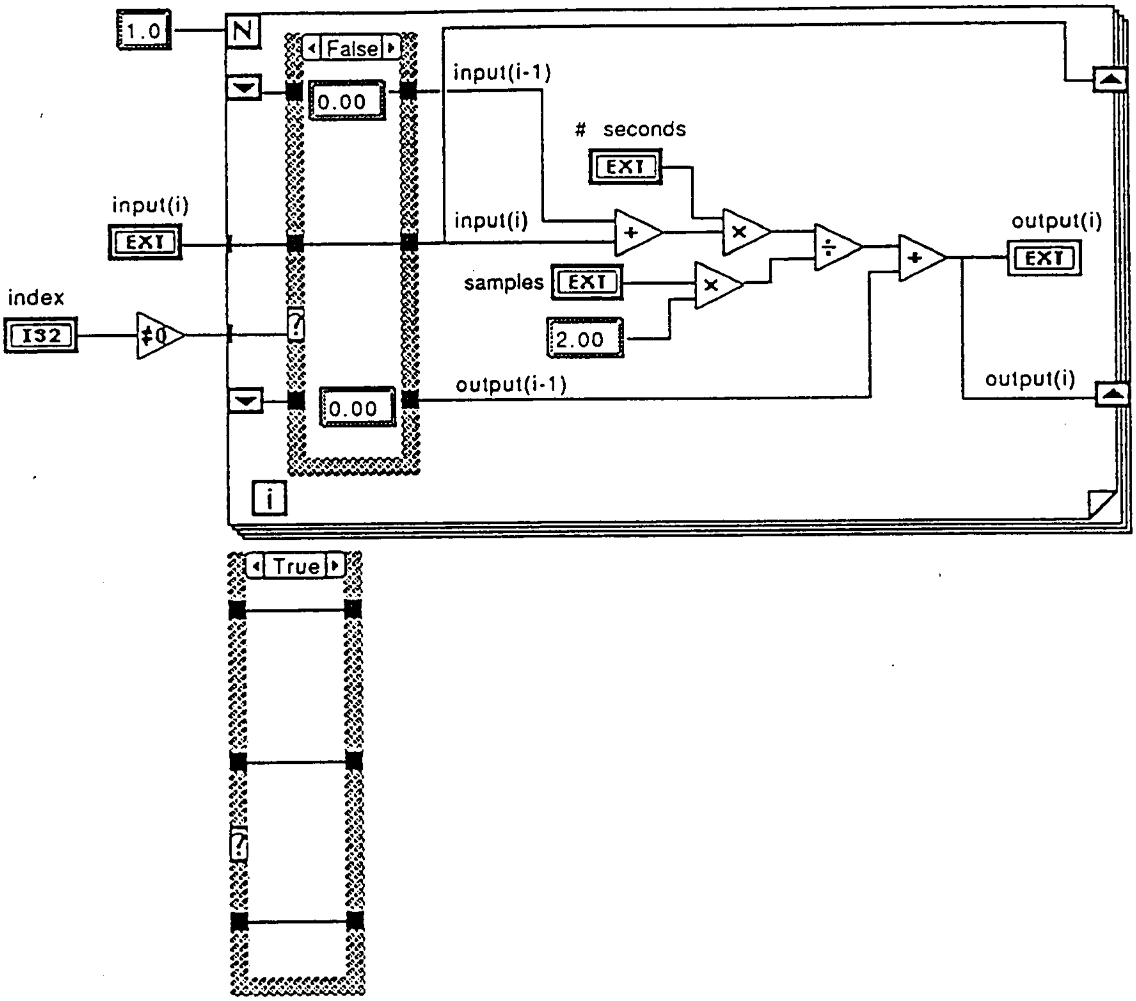

Figure 4.0-4. Integrator Subroutine

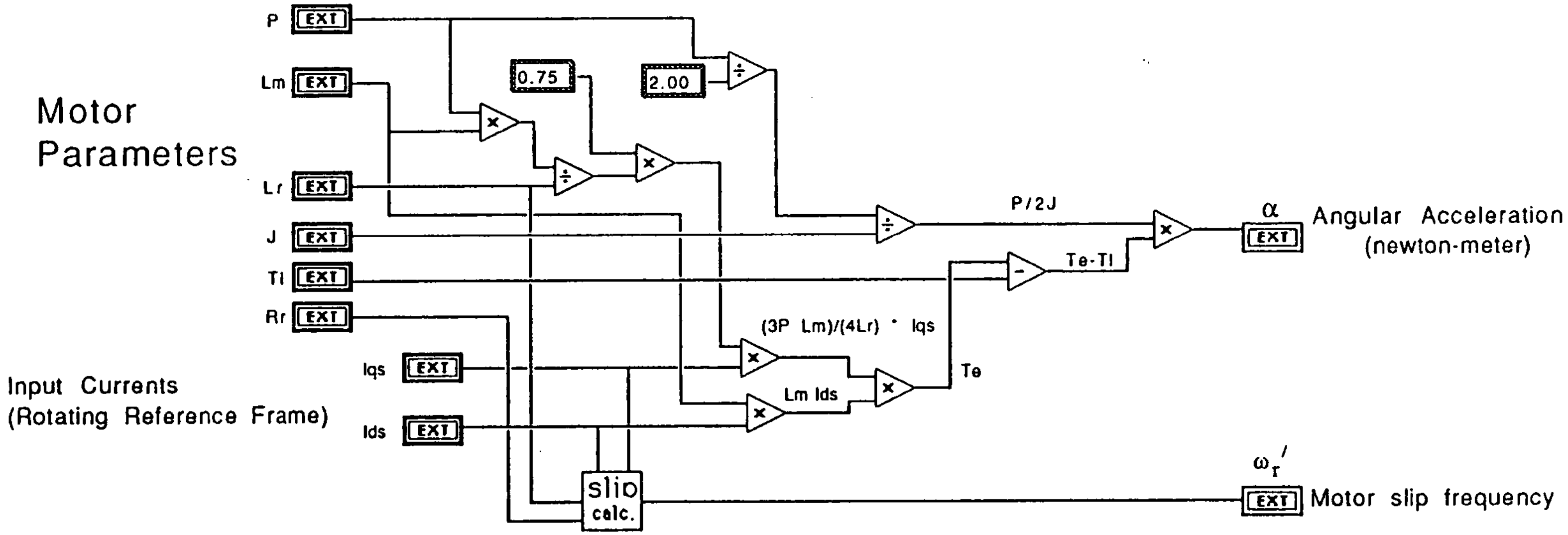

Figure 4.0-5. Steady State Induction Motor Model

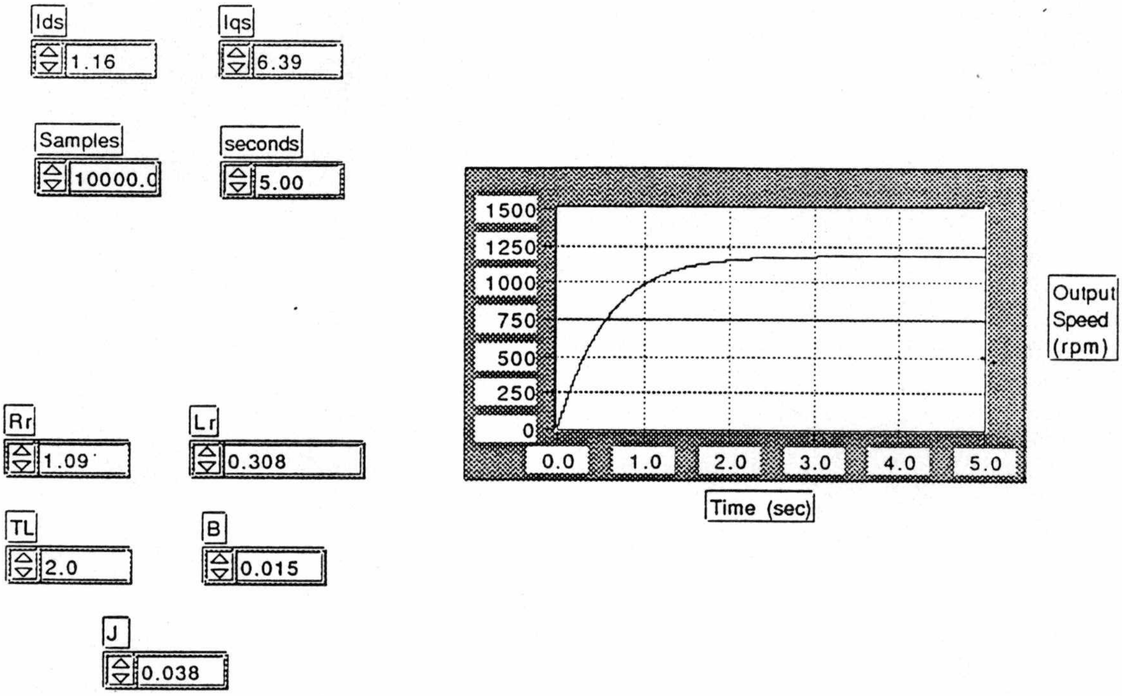

Figure 4.0-6. Simulation with $i_{ds}=1.16$ amps and $i_{qs}=6.39$ amps

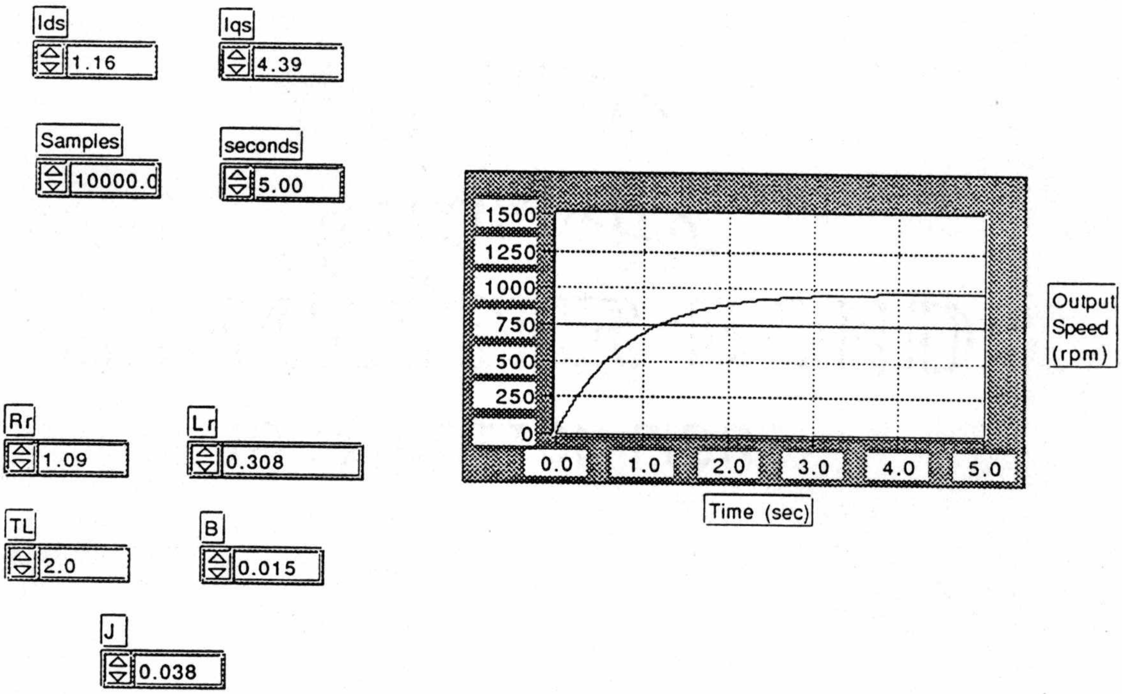

Figure 4.0-7. Simulation with $i_{ds}=1.16$ amps and $i_{qs}=4.39$ amps

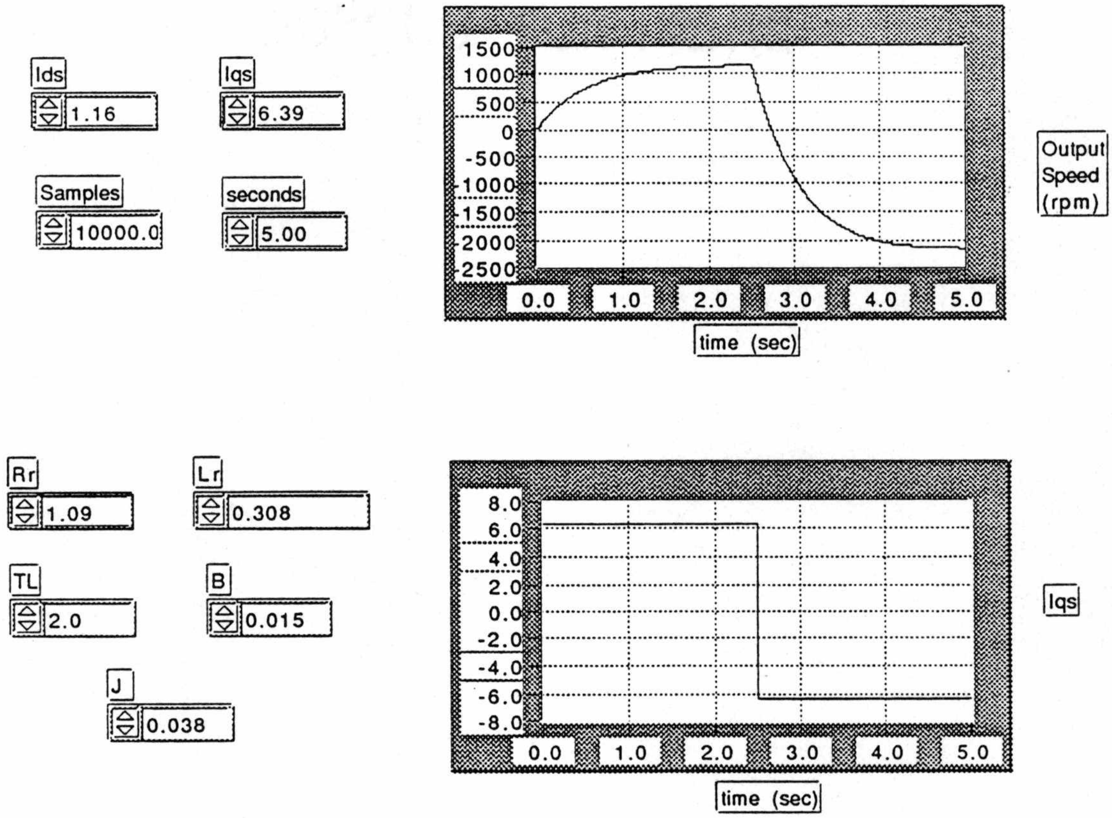

Figure 4.0-8. Simulation with $i_{ds}=1.16$ amps and Varying i_{qs}

VITA

Richard B. Smith was born in Nashville, Tennessee on June 29, 1958. He attended Elementary, Junior High, and High schools in Nashville, Tennessee and graduated from Hillsboro High School in June, 1976. The following September he enrolled in Tennessee Technological University. He received the degree of Bachelor of Science in Electrical Engineering in June of 1981. He was then employed as an Electrical Engineer in the Test Engineering and Athens Division Substation Test Departments of Georgia Power Company where he became registered as a Professional Engineer in the state of Georgia. He entered the University of Tennessee, Knoxville in August, 1989 and in May 1992, received a Master of Science degree in Electrical and Computer Engineering. He is presently employed as a Power Quality Engineer at the Tennessee Center for Research and Development, Knoxville, Tennessee.